ACS APPLIED MATERIALS & INTERFACES

Letter

www.acsami.org

Fabrication of Hydrogel with Cell Adhesive Micropatterns for Mimicking the Oriented Tumor-Associated Extracellular Matrix

Zhaobin Guo,[†,‡] Ke Hu,[†,‡] Jianfei Sun,[†] Tianzhu Zhang,*[,†,‡] Qiying Zhang,[†] Lina Song,[†] Xizhi Zhang,[†] and Ning Gu*[,†,‡]

[†]State Key Laboratory of Bioelectronics and Jiangsu Key Laboratory for Biomaterials and Devices, School of Biological Science and Medical Engineering & Collaborative Innovation Center of Suzhou Nano Science and Technology, Southeast University, Sipailou 2, Nanjing 210096, People's Republic of China

[‡]Suzhou Key Lab of Biomedical Materials and Technology, Research Institute of Southeast University in Suzhou, Ren Ai Road 150, Suzhou Industrial Park, Suzhou 215123, China

Supporting Information

ABSTRACT: For mimicking the fibrous extracellular matrix (ECM), a facile method for patterning anticell adhesive substrate was novelly applied on agarose hydrogel. Without using masks or templates for etching, we applied the magnetic field-induced colloidal assembly of magnetic nanoparticles on the flat agarose hydrogel to form cell-adhesive micropatterns. Meanwhile, tuning the hydrogel substrate's modulus to fit real tissue was experimentally demonstrated. Magnetic nanobeads were also assembled on this hydrogel surface and formed more complete and regular patterns. The patterned hydrogel substrate could actually influence behaviors of different cancer cells, including adhesion, growth, and migration.

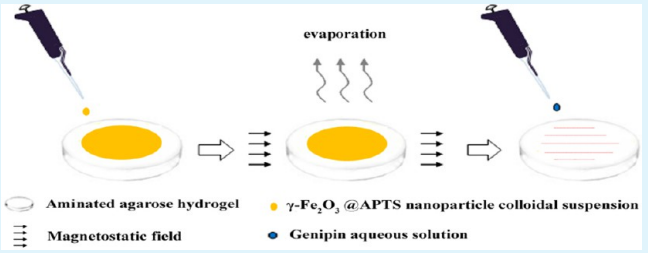

KEYWORDS: *magnetostatic field induced assembly, magnetic nanomaterials, cell-adhesive micropatterns, agarose hydrogel, tumor-associated ECM*

Cellular microenvironments, which commonly refer to the places where cells reside, provide not only physical supports and signal transduction but also anchoring sites which can maintain cell migration and prevent anoikis.[1−5] Cellular microenvironments consist of cellular parts and acellular parts; the former include various kinds of cells, such as mesenchymal cells, immunocyte, or endothelial cells, and the latter are mainly the substrates like extracellular matrix (ECM). Recently, increasing attention has been paid to the physical factors of cellular microenvironment.[6,7] It has been reported that both "bulk" (e.g., mechanical and chemical properties) and "interfacial" (e.g., interfacial energy, topography, etc.) properties affect the differentiation of stem cells or the motility of both normal and cancer cells.[8−10] Since the cellular microenvironments are sophisticated, the integration of these factors is possible to be an effective method to replicate the cellular microenvironment, which can make cell behaviors in vitro similar to those in vivo.[11−13]

The patterning of the cell-contact interface, whether physical or chemical, is one of the central issues in the study of cell behaviors. For example, by using hard lithography, such as photo- or laser-lithography, surfaces with patterns of different shape and scale have been prepared to study cell morphology as well as adhesion, migration, and differentiation.[14−19] Meanwhile, soft lithography is also extensively investigated. Through patterning "inks", such as protein-absorbed molecules, or protein itself, on interfaces, researchers are allowed to modify the substrate interface on the scale of micrometers.[20−25] Topographically, the as-prepared patterns, which are known as "top-down", are of great regularity. However, naturally formed ECM does not have regularity in such a high degree. In fact, normal ECM consists of matrices with nondirectional arrangements, while tumor-associated ECM arranged orderly. As shown in Amatangelo et al.'s report, tumor-associated fibroblasts could produce matrices with an apparently progressive parallel arrangement, which is greatly different from the chaotic structure of the normal matrix.[26] According to previous work in our group, the assembly of magnetic nanoparticles induced by the magnetic field could produce orderly fibrous patterns on rigid substrates (silicon, glass, etc.).[27] Owing to the resemblance between these patterns and tumor-associated ECM in topography, this assembly technique might be a good candidate in mimicking tumor-associated ECM.

Herein, we address this issue by a simple and versatile method. Cell-adhesive nanomaterials were assembled into parallelly arranged patterns on the surface of anticell adhesive hydrogel with appropriate mechanical properties, which consider topography, mechanical properties, and cell-adhesive

Received: April 23, 2014
Accepted: July 3, 2014
Published: July 3, 2014

 © 2014 American Chemical Society

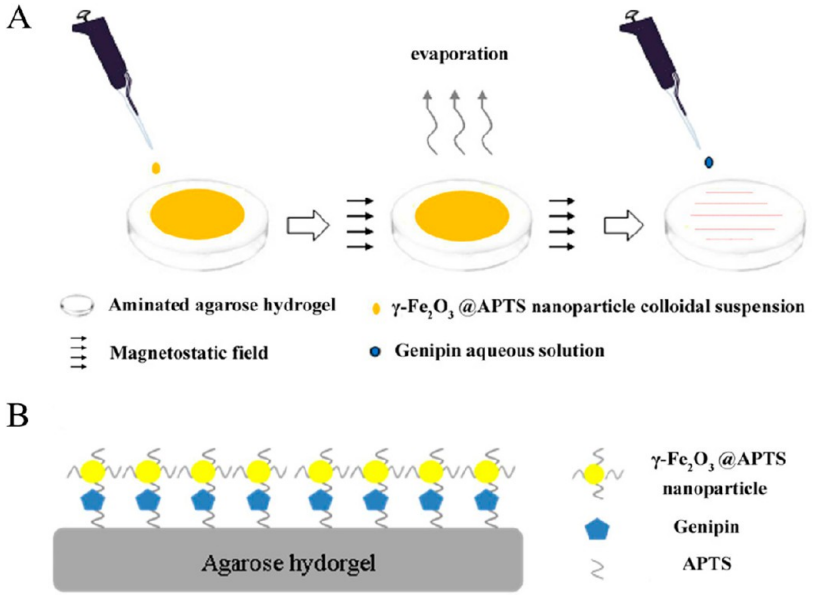

Figure 1. (A) Schematic illustration of the basic steps of fabricating micropatterns on agarose hydrogel substrate and (B) a schematic illustration of covalently binding of γ-Fe_2O_3@APTS MNPs by genipin on the hydrogel substrate.

function integratively (Figure 1). To improve the stabilization of the patterns, in other words, to prevent patterns from shedding off from the hydrogel surface when used for cell culture, they were tethered on the surface of the hydrogel by the biocompatible reagent genipin. Through preparing the hydrogel, we demonstrated that cell-adhesive patterns on the soft interface with mimicking real tissue affected the adhesion and migration of ovarian cancer cells.

The impact of the mechanical properties of substrate on cell behaviors has been extensively studied, but the substrate employed mostly was poly(acryamide) (PAM) hydrogel.[6,7] Through changing the ratio of monomers (i.e., acrylamide, AM) to cross-linkers (e.g., *N*,*N*′-methylenebis(acrylamide), or BIS), the mechanical properties of hydrogel could be tuned. However, when cells were cultured on this kind of hydrogel, the residue of the initiator (ammonium persulfate, APS) or cross-linker BIS might lead to the microenvironments more different from those in vivo; in addition, the toxicity of monomer might even aggravate this problem.[28] Therefore, we selected agarose hydrogel as the substate material because of its high biocompatibility. Meanwhile, the function of formed micropatterns could be remarkably distinguished from hydrogel substrate owing to the antiadhesiveness of agarose hydrogel.

Moreover, the modulus of substrate can be conveniently tuned in a wide range, only by varying the concentration of agarose solution. Figure 2 shows the Young's modulus (E) of hydrogels containing 0.3%, 0.5%, 0.8%, 1.0%, 1.5%, and 2.0% (w/w) of agarose (named as hydrogel 0.3, hydrogel 0.5, hydrogel 0.8, hydrogel 1.0, hydrogel 1.5, and hydrogel 2.0, respectively, in this paper). The Young's moduli of hydrogel 1.0 and hydrogel 0.3 are 15.556 ± 1.298 kPa and 3.664 ± 0.646 kPa, respectively.

According to Engler, the physiological modulus of muscle tissue and brain tissue varies from 8 to 17 kPa and 0.1 to 1 kPa, respectively.[7] Therefore, we could conclude that the Young's modulus of hydrogel 1.0 and hydrogel 0.3 is closer to those of muscle and brain. Then by forming hydrogels on silicon wafers, the flat hydrogel surface can be obtained, which could reduce the disturbance of the assembling process.

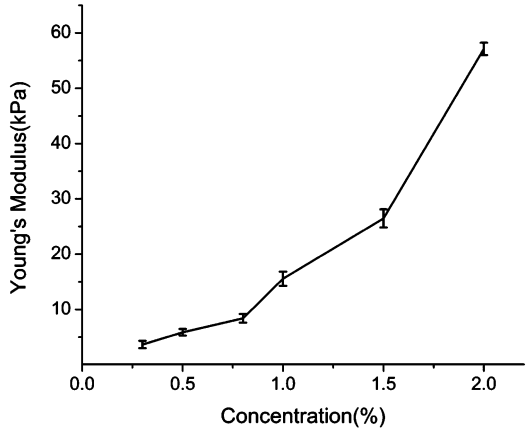

Figure 2. Young's modulus of agarose hydrogels (content of agarose are 0.3%, 0.5%, 0.8%, 1.0%, 1.5%, and 2% (w/w), respectively).

3-Amino-propyltriethoxysilane (APTS) coated γ-Fe_2O_3 magnetic nanoparticles (γ-Fe_2O_3@APTS MNPs) (average size 7.5 nm, average hydrodynamic size 82.9 nm, Supporting Information Figure S1) were assembled on hydrogel to form cell adhesive patterns. Although this assembly of nanoparticles is mature to fabricate patterns on rigid substrates, such as silicon, glass, etc., few researchers have used this technique to pattern soft and high water content substrates. When this technique was transplanted to a patterned surface with a high fraction of water mass, the micropattern shed easily from the hydrogel during cell culturing, which made the cells and cell aggregates that first adhered to and migrated on the substrate separate from it within a few days. In order to fix this problem, an approach was used to immobilize the patterns: the surface of agarose hydrogel was first aminated with the silane coupling agent 3-amino-propyltriethoxysilane (APTS), and then the amino groups of APTS were conjugated both on hydrogel and γ-Fe_2O_3@APTS MNPs by a biocompatible reagent, genipin, which is an alternative to the cell-toxic glutaraldehyde (GA).

The morphologies of the fibrous and mesh-like γ-Fe_2O_3@APTS MNPs patterns were characterized through optical

dx.doi.org/10.1021/am5023946 | ACS Appl. Mater. Interfaces 2014, 6, 10963−10968

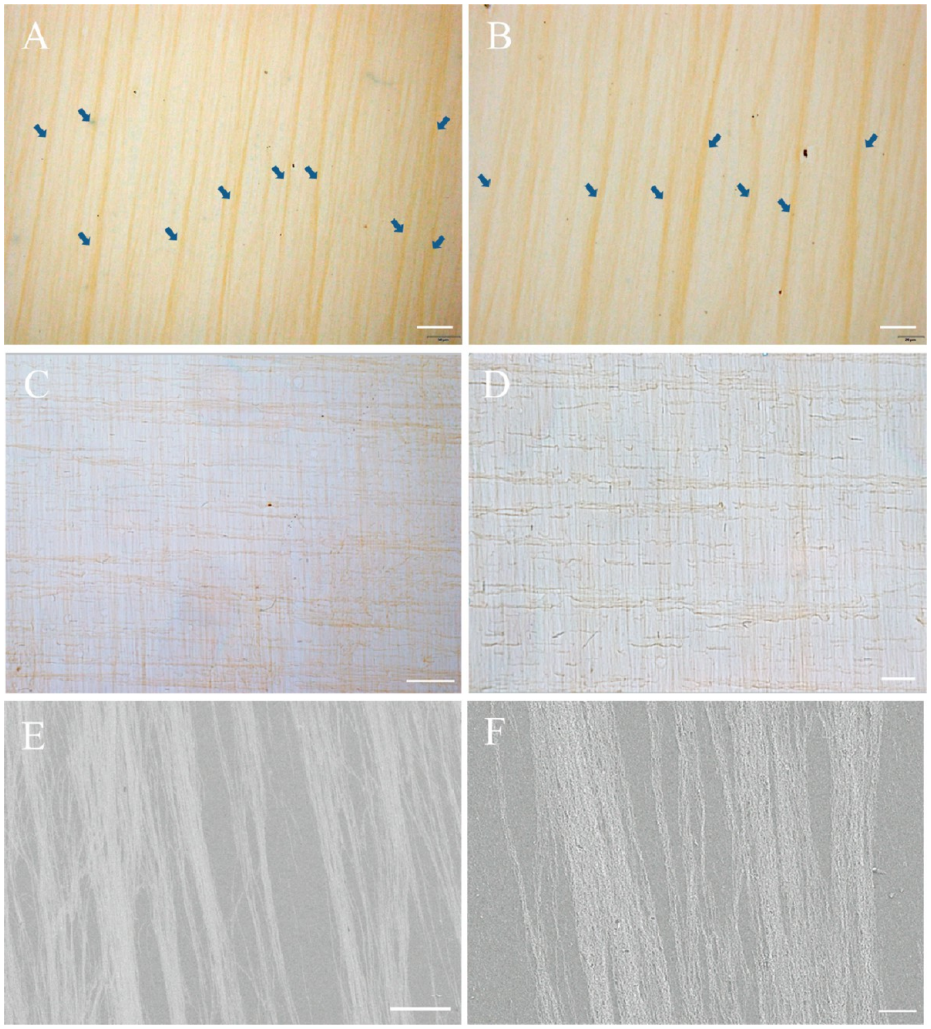

Figure 3. (A–D) Optical microscope images of γ-Fe_2O_3@APTS MNPs assembled fibrous and mesh-like structure which were patterned under magnetic field once (A and B) or twice (C and D). Scale bar in (A) and (C): 50 μm, (B) and (D) 20 μm. (E, F) SEM images of the fibrous structure on silicon wafer. Scale bar in (E), 20 μm, and (F), 5 μm.

microscope, as presented in Figure 3A–D. Scanning electron microscope (SEM) images are shown in Figure 3E,F. In Figure 3A,B, we can observe the formed patterns consisting of wider fibers (indicated by blue arrows) or narrower fibers (indicated by green arrows). The widths of the wider fibers are measured as 5.26 ± 1.91 μm in Figure 3A (10 fibers marked by blue arrows) and 4.58 ± 0.67 μm in Figure 3B (7 fibers marked by blue arrows), which proves that the width of the line is about 1–10 μm. However, because of the relatively low resolution of the microscope, SEM is also employed to characterize the patterns which assembled on silicon wafers (Figure 3E,F). The SEM images showed that fibers in the microscale consist of densely arranged fibers in the hundred-nanometer scale, which is similar to the ECM structure where a great number of nanoscale collegen fibers self-assembled to microscale fibers.

Polystyrene magnetic nanobeads (PS MBs) (average hydrodynamic size 269.6 nm, see Supporting Information Figures S2 and 3S) were also assembled on hydrogel substrates, in order to prove the versatility of our method in fabricating micropatterns with nanomaterials of different size, magnetism, or composites.

By using PS MBs as building blocks, fiber-like patterns also were formed on the agarose hydrogel surface (Figure 4A,B). The width of the line in Figure 4D is 4.32 ± 1.37 μm, which proved that fibers assembled by PS MBs and γ-Fe_2O_3@APTS MNPs do not have significant differences. However, patterns formed by PS MBs are of regularity higher than that of γ-Fe_2O_3@APTS MNPs patterns. This might be explained by the following reasons: because the single PS MB (encapsulates several Fe_3O_4 MNPs in one PS MB) could be considered as an aggregation of Fe_3O_4 MNPs, it might be driven by magnetic field more easily than a single magnetic nanoparticle. Thus, PS MBs were more easily recruited as building blocks of micropatterns. In fact, the matastability of the nanoparticle is necessary for assembly. Therefore, the nanoparticles we used are without stabilizing agents, and nanoparticle clusters are formed in the suspension (hydrodynamic size 82.9 nm). However, the random aggregation of MNPs leads to the well dispersed single nanoparticle, small clusters, and relatively bigger clusters that coexisted in suspension. Therefore, a number of well dispersed γ-Fe_2O_3@APTS MNPs remained static or are less motivated to assemble.

The SEM images supported this inference. PS MBs performed a complete assembly (Figure 4C,D), but γ-Fe_2O_3@APTS MNPs were distributed throughout on silicon wafer (Figure 3E,F), and the boundary of the fibers could not be identified as clearly as PS MBs formed fibers. Meanwhile, the

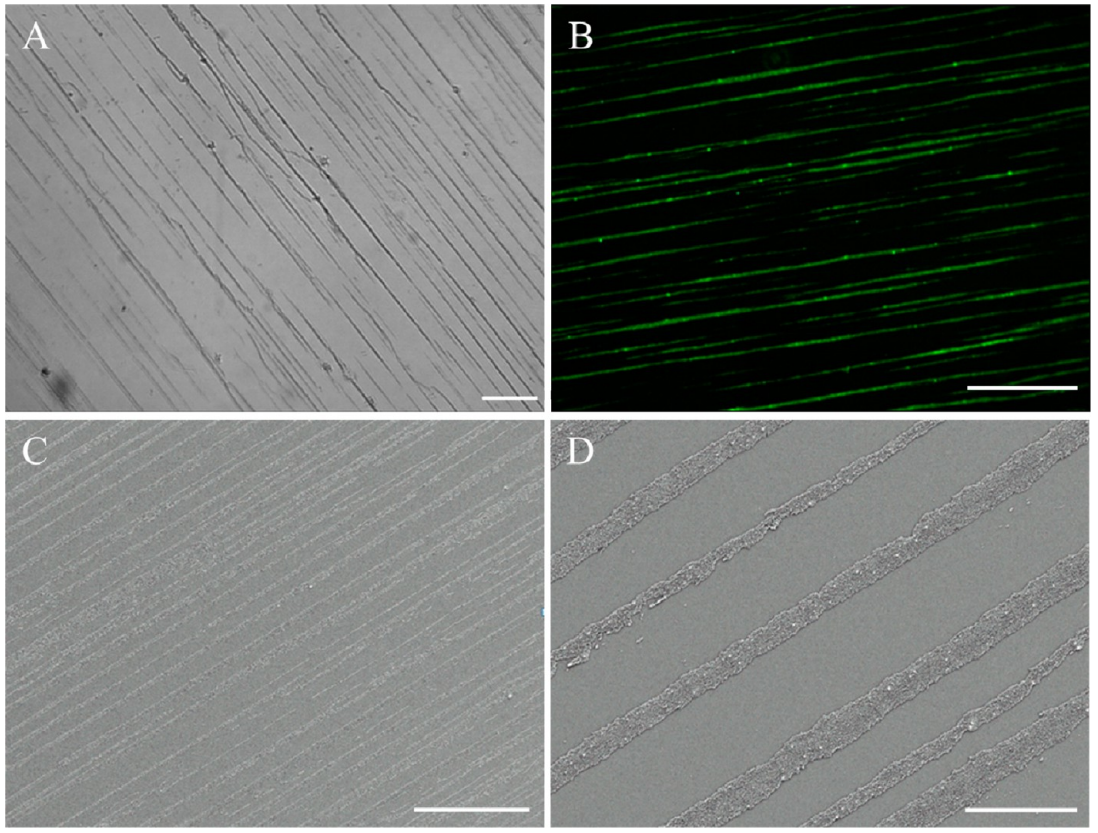

Figure 4. (A, B) optical microscope images of PS MBs assembled patterns. Scale bar in (A): 100 μm. (B) Florescent image of patterns assembled by FITC labeled PS MBs. Scale bar in (B): 25 μm. (C, D) SEM images of PS MBs patterns on silicon wafer. Scale bar in (C): 10 μm. Scale bar in (D): 5 μm.

larger size and stronger magnetic dipolar−dipolar interaction make PS MB assemblies more stable against disturbance during the evaporating process. And the assembling process does not change the superhydropilicity of the interface (0° of water contact angle, see A3 and B3 in Supporting Information Figure 4S) although it slightly decreases the rate of spreading of the water droplet (see A2 and B2 in Supporting Information Figure 4S). This might be due to a little interference of spreading of water induced by the patterns rather than the change of the hydrophilicity of the interface.

In order to more clearly characterize the topography of PS MBs patterns, PS MBs were first absorbed with FITC labeled bovine serum albumin (BSA), and then florescent images were taken. After mixing PS MBs with FITC labeled bovine serum albumin (BSA), the fibrous structures were clearly visualized (Figure 4B), which proved that the amount of absorbed protein on PS MBs was quite large. Therefore, we might predict that, by absorbing ECM proteins from culture medium or cells themselves, micropatterns consisting of PS MBs would promote cell adhesion.

After the initial plating in 100 μL of the culture medium for 30 min, most cells adhered to the patterned surface of the hydrogel. Few cells dropped off when they underwent a gentle shaking. A time-lapsed microscope was then used to observe cells (see Supporting Information, S1 mov.). After culturing for 6 h (Figure 5A), most cells were elongated and some had an oriented elongation in a direction consistent with the patterns (indicated by blue arrows). At 12 h in culture (Figure 5B), the number of cells that were elongated in a direction consistent with the patterns (indicated by blue arrows) had increased. Another ovarian cancer cell line, SKOV-3, cultured on patterns, performed a similar elongation of cells when cultured for 24 h (Figure 6A) and 48 h (Figure 6B). Supporting Information Figure 5S showed the orientated spreading of osteoblasts MC3T3 on γ-Fe_2O_3@APTS MNP patterns on silicon wafer, where the angles between the cells and fibers are about 9.7° ± 0.2° after 24 h of culturing. We therefore can conclude that the fabricated patterns on substrate thus had the capacity to orient the spread of cells, which also means that γ -Fe_2O_3@APTS MNPs possessed the capacity to adhere to cells. Therefore, these patterns formed on agarose hydrogel in a magnetostatic field mimicked ECM not only from structures but also from cell-adhesion function to a certain extent.

The video (Supporting Information S1 mov.) further demonstrated that most cells had a tendency to migrate along with fibrous patterns. These may be in agreement with the possibility that the cell migration was partly guided by the fabricated pattern. As reported in previous studies, some cancer cell lines are able to form cell aggregates or multicellular spheroids when they are placed in microenvironments with a limited cell−matrix adhesion function, such as scaffolds constructed by electrospinning or stimuli-responsive hydrogels, which forced cells to contact each other and then increased cell−cell interactions.[29,30] In fact, the video also demonstrated that some cells approached and even attached to each other to form aggregates (indicated by blue arrows in Figure 5C), although not typical multicellular spheriods. This might be due to, as mentioned above, that the cell−matrix interactions were not limited sufficiently. Hence the patterned interface might potentially be used to produce multicellular spheroids when

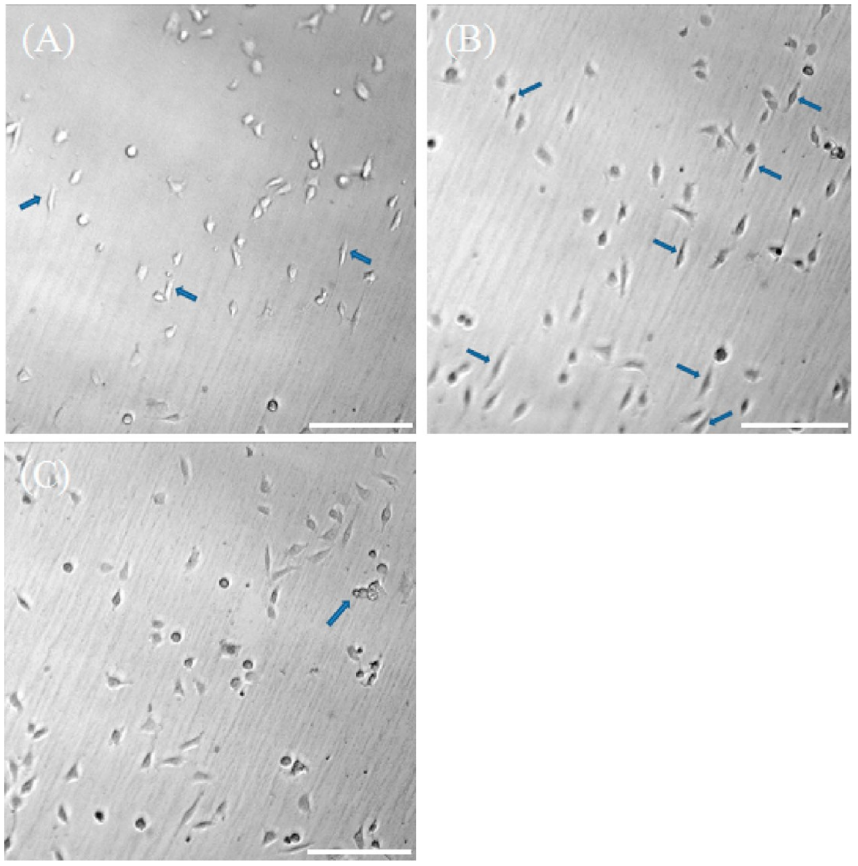

Figure 5. Morphology, migration, and tendency of aggregation of OVCAR-5 cells on micropatterned γ-Fe_2O_3@APTS MNPs agarose hydrogels. (A and B) Morphology of cells after culturing for 6 h and 12 h, respectively. Blue arrows point the oriented elongating of cells by micropatterns. (C) Tendency of cell migrating to form aggregation after culturing for 24 h. Blue arrows point to the tendency of cells aggregation. Scale bar: 100 μm.

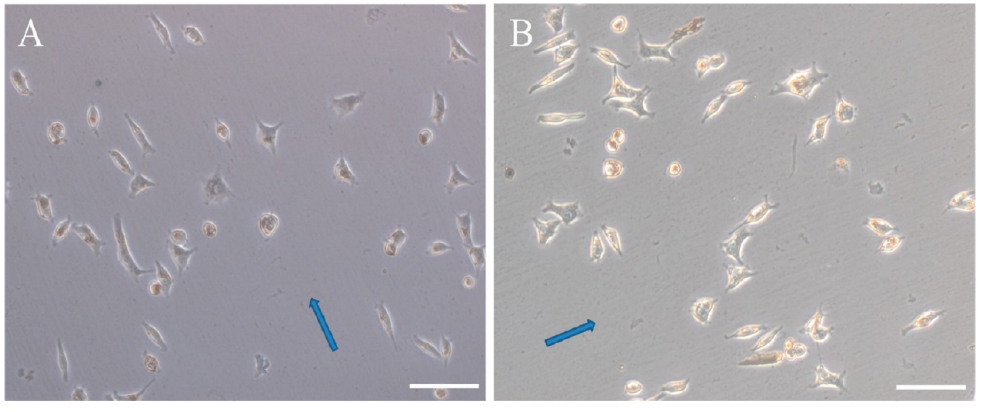

Figure 6. Morphology and oriented elongating of SKOV-3 cells on micropatterned γ-Fe_2O_3@APTS MNPs agarose hydrogels after cultured for 24 h (A) and 48 h (B), respectively. Blue arrows indicate the direction of micropatterns. Scale bar: 100 μm.

cell−matrix interactions were decreased. This could be achieved by controlling the width of a single microscale fiber in patterns and the spaces between the adjacent fibers, depending on the quantity of assembled nanomaterials and the intensity of the magnetic field.

Overall, to mimick tumor-associated ECM from fibrous structures and cell-adhesive functions, we provided a novel method to obtain mechanically tissue-like agarose hydrogel substrate with microscale, cell-adhesive patterns on the interface. Directed by a magnetostatic field, magnetic nanomaterials, such as γ-Fe_2O_3@APTS MNPs or PS MBs, could be assembled into either fibrous or mesh-like micropatterns. Both of them were easily fabricated on soft and high water-content agarose hydrogel, which avoided the use of masks or templates for etching. In addition, the patterns not only promoted the adhesion of cells and guided their migration but also showed the potential to promote the aggregation of ovarian cancer cells.

■ ASSOCIATED CONTENT

Ⓢ Supporting Information

Time lapsed video of cell culturing, SEM images, and hydrodynamic sizes of γ-Fe_2O_3@APTS MNPs and PS MBs, thermogravimetric analysis of PS MBs, water contact angles of hydrogel before and after patterning, and SEM images of

MC3T3 osteoblasts cultured on patterns. This material is available free of charge via the Internet at http://pubs.acs.org/.

AUTHOR INFORMATION

Corresponding Authors

*(T.Z.) Fax: +86 25 83272460. E-mail: zhangtianzhu@seu.edu.cn.

*(N.G.) Fax: +86 25 83272460. E-mail: guning@seu.edu.cn.

Notes

The authors declare no competing financial interest.

ACKNOWLEDGMENTS

We acknowledge the support of the National Basic Research Program of China (2011CB933503), the Special Project on Development of National Key Scientific Instruments Equipment of China (2011YQ03013403), National Natural Science Foundation of China (NSFC 21273002), and Jiangsu Provincial Special Program of Medical Science (BL2013029). T.Z.Z. is grateful for supports from the program for New Century Excellent Talents in University (NCET-09-0298), and J.F.S. is thankful for supports from National Natural Science Foundation of Jiangsu Province (BK2011590). K.H. is also grateful for supports from the research innovation plan of colleges and universities postgraduates of Jiangsu Province (CXLX12_0120). The authors also thank Ms. Naizhen Zhou for cell culturing.

REFERENCES

(1) Cukierman, E.; Pankov, R.; Yamada, K. M. Cell Interactions with Three-dimensional Matrices. *Curr. Opin. Cell Biol.* **2002**, *14*, 633−639.

(2) Fuchs, E.; Tumbar, T.; Guasch, G. Socializing with the Neighbors: Stem Cells and Their Niche. *Cell* **2004**, *116*, 769−778.

(3) Guilak, F.; Cohen, D. M.; Estes, B. T.; Gimble, J. M.; Liedtke, W.; Chen, C. S. Control of Stem Cell Fate by Physical Interactions with the Extracellular Matrix. *Cell Stem Cell* **2009**, *5*, 17−26.

(4) Schmeichel, K. L.; Bissell, M. J. *J.* Modeling Tissue-Specific Signaling and Organ Function in Three Dimensions. *Cell Sci.* **2003**, *116*, 2377−2388.

(5) Cukierman, E.; Pankov, R.; Stevens, D. R.; Yamada, K. M. Taking Cell-Matrix Adhesions to the Third Dimension. *Science* **2001**, *294*, 1708−1712.

(6) Engler, A.; Bacakova, L.; Newman, C.; Hategan, A.; Griffin, M.; Discher, D. Substrate Compliance Versus Ligand Density in Cell on Gel Responses. *Biophys. J.* **2004**, *86*, 617−628.

(7) Engler, A. J.; Sen, S.; Sweeney, H. L.; Discher, D. E. Matrix Elasticity Directs Stem Cell Lineage Specification. *Cell* **2006**, *126*, 677−689.

(8) Sung, J. H.; Yu, J. J.; Luo, D.; Shuler, M. L.; March, J. C. Microscale 3-D Hydrogel Scaffold for Biomimetic Gastrointestinal (GI) Tract. Model. *Lab Chip* **2011**, *11*, 389−392.

(9) DeForest, C. A.; Anseth, K. S. Photoreversible Patterning of Biomolecules within Click-Based Hydrogels. *Angew. Chem., Int. Ed.* **2012**, *51*, 1816−1819.

(10) Ayala, R.; Zhang, C.; Yang, D.; Hwang, Y.; Aung, A.; Shroff, S. S.; Arce, F. T.; Lal, R.; Arya, G.; Varghese, S. Engineering the Cell-material Interface for Controlling Stem Cell Adhesion, Migration, and Differentiation. *Biomaterials* **2011**, *32*, 3700−3711.

(11) Higuchi, A.; Ling, Q. D.; Hsu, S. T.; Umezawa, A. Biomimetic Cell Culture Proteins as Extracellular Matrices for Stem Cell Differentiation. *Chem. Rev.* **2012**, *112*, 4507−4540.

(12) Tibbitt, M. W.; Anseth, K. S. Hydrogels as Extracellular Matrix Mimics for 3D Cell Culture. *Biotechnol. Bioeng.* **2009**, *103*, 655−663.

(13) Loessner, D.; Stok, K. S.; Lutolf, M. P.; Hutmacher, D. W.; Clements, J. A.; Rizzi, S. C. Bioengineered 3D Platform to Explore Cell-ECM Interactions and Drug Resistance of Epithelial Ovarian Cancer Cells. *Biomaterials* **2010**, *31*, 8494−8506.

(14) Engelmayr, G. C., Jr.; Cheng, M.; Bettinger, C. J.; Borenstein, J. T.; Langer, R.; Freed, L. E. Accordion-like Honeycombs for Tissue Engineering of Cardiac Anisotropy. *Nat. Mater.* **2008**, *7*, 1003−1010.

(15) Beduer, A.; Vieu, C.; Arnauduc, F.; Sol, J. C.; Loubinoux, I.; Vaysse, L. Engineering of Adult Human Neural Stem Cells Differentiation through Surface Micropatterning. *Biomaterials* **2012**, *33*, 504−514.

(16) Yoshii, Y.; Waki, A.; Yoshida, K.; Kakezuka, A.; Kobayashi, M.; Namiki, H.; Kuroda, Y.; Kiyono, Y.; Yoshii, H.; Furukawa, T.; Asai, T.; Okazawa, H.; Gelovani, J. G.; Fujibayashi, Y. The Use of Nano-imprinted Scaffolds as 3D Culture Models to Facilitate Spontaneous Tumor Cell Migration and Well-regulated Spheroid Formation. *Biomaterials* **2011**, *32*, 6052−6058.

(17) Krsko, P.; McCann, T. E.; Thach, T. T.; Laabs, T. L.; Geller, H. M.; Libera, M. R. Length-scale Mediated Adhesion and Directed Growth of Neural Cells by Surface-patterned Poly(ethylene glycol) Hydrogels. *Biomaterials* **2009**, *30*, 721−729.

(18) Song, W.; Kawazoe, N.; Chen, G. J. Dependence of Spreading and Differentiation of Mesenchymal Stem Cells on Micropatterned Surface Area. *J. Nanomater.* **2011**, *2011*, 1−9.

(19) Slater, J. H.; Miller, J. S.; Yu, S. S.; West, J. L. Fabrication of Multifaceted Micropatterned Surfaces with Laser Scanning Lithography. *Adv. Funct. Mater.* **2011**, *21*, 2876−2888.

(20) Solanki, A.; Shah, S.; Memoli, K. A.; Park, S. Y.; Hong, S.; Lee, K. B. Controlling Differentiation of Neural Stem Cells Using Extracellular Matrix Protein Patterns. *Small* **2010**, *6*, 2509−2513.

(21) Wei Luo, S. R. J.; Muhammad, N. Yousaf. Geometric Control of Stem Cell Differentiation Rate on Surfaces. *Langmuir* **2008**, *24*, 12129−12133.

(22) Connelly, J. T.; Gautrot, J. E.; Trappmann, B.; Tan, D. W.; Donati, G.; Huck, W. T.; Watt, F. M. Actin and Serum Response Factor Transduce Physical Cues from the Microenvironment to Regulate Epidermal Stem Cell Fate Decisions. *Nat. Cell Biol.* **2010**, *12*, 711−719.

(23) Tay, C. Y.; Yu, H.; Pal, M.; Leong, W. S.; Tan, N. S.; Ng, K. W.; Leong, D. T.; Tan, L. P. Micropatterned Matrix Directs Differentiation of Human Mesenchymal Stem Cells Towards Myocardial Lineage. *Exp. Cell Res.* **2010**, *316*, 1159−1168.

(24) Damljanovic, V.; Christoffer Lagerholm, B.; Jacobson, K. Bulk and Micropatterned Conjugation of Extracellular Matrix Proteins to Characterized Polyacrylamide Substrates for Cell Mechanotransduction Assays. *Biotechniques* **2005**, *39*, 847−851.

(25) Tang, X.; Ali, M. Y.; Saif, M. T. A Novel Technique for Micro-Patterning Proteins and Cells on Polyacrylamide Gels. *Soft Matter* **2012**, *8*, 7197−7206.

(26) Amatangelo, M. D.; Bassi, D. E.; Klein-Szanto, A. J. P.; Cukierman, E. Stroma-Derived Three-Dimensional Matrices Are Necessary and Sufficient to Promote Desmoplastic Differentiation of Normal Fibroblasts. *Am. J. Pathol.* **2005**, *167*, 475−488.

(27) Sun, J. F.; Zhang, Y.; Chen, Z. P.; Zhou, H.; Gu, N. Fibrous Aggregation of Magnetite Nanoparticles Induced by a Time-Varied Magnetic Field. *Angew. Chem., Int. Ed.* **2007**, *46*, 4767−4770.

(28) Xi, T. F.; Fan, C. X.; Feng, X. M.; Wan, Z. Y.; Wang, C. R.; Chou, L. L. Cytotoxicity and Altered C-myc Gene Expression by Medical Polyacrylamide Hydrogel. *J. Biomed. Mater. Res., Part A* **2006**, *78A*, 283−290.

(29) Feng, Z. Q.; Chu, X. H.; Huang, N. P.; Wang, T.; Wang, Y. C.; Shi, X. L.; Ding, Y. T.; Gu, Z. Z. The Effect of Nanofibrous Galactosylated Chitosan Scaffolds on the Formation of Rat Primary Hepatocyte Aggregates and the Maintenance of Liver Function. *Biomaterials* **2009**, *30*, 2753−2763.

(30) Wang, D. D.; Cheng, D.; Guan, Y.; Zhang, Y. J. Thermoreversible Hydrogel for In Situ Generation and Release of HepG2 Spheroids. *Biomacromolecules* **2011**, *12*, 578−584.